Evaluation of Pulsed Laser Holograms of Flashing Sprays by Digital Image Processing and Holographic Particle Image Velocimetry

O. Feldmann, P. Gebhard, F. Mayinger, Lehrstuhl A für Thermodynamik, Technische Universität München, 85747 Garching, Germany

ABSTRACT

This study deals with the application of the pulsed laser holography and the digital image processing in the analysis of flashing sprays. Both the information about the macroscopic structures of a spray, such as the breakup-length and the spray-angle, and about its microscopic structures, such as the number, the size, and the location of the generated droplets is stored three-dimensionally on a single pulsed hologram. In addition to that, the velocity of the droplets can be obtained from double pulsed holograms. In every experiment, two holograms are taken, resulting in two three-dimensional reconstructions of the test section, seen from different directions. These reconstructions are scanned by video-cameras with a small depth of field and subdivided into several two-dimensional images. These images are digitized and binarized, and the information about the droplets depicted sharply on each image is saved. In case of a double pulsed hologram, a Fourier-analysis based algorythm creates a search volume to detemine the droplets' second position and thus their velocity in each view. A stereomatching modulus correlates both views and determines the position and/or the velocity of each droplet highly accurate. The applicability of the employed holographic technique and the filtering and correlating moduli is proven by the presented results.

Keywords: Holography, Flow Visualization, Particle Size, Phase Velocities, Spray, Flashing

INTRODUCTION

In many technical applications sprays play an important part. Sprays can be formed by:

- mechanical disintegration of the liquid due to shear forces and induced turbulence,
- and thermodynamic disintegration by flashing of the liquid.

Especially in the field of fuel injection and because of safety aspects in process engineering the disintegration of a liquid jet by flashing is an interesting phenomenon. This paper reports on a study of sprays generated by injecting subcooled or superheated liquid through flat spray pressure nozzles. 'Superheated' in this case means that the liquid temperature is higher than its saturation temperature corresponding to the pressure in the test chamber the liquid is injected in. Injecting superheated liquid, its fragmentation is caused by both mechanical forces and the growing of vapour bubbles in the metastable part of the liquid veil. The pulsed laser holography was applied to analyze the spray.

In the last 15 years many efforts have been made to evaluate pulsed laser holograms of particle fields by applying techniques of the digital image processing. An insight into this problem was presented by HAUSSMANN & LAUTERBORN [4]. Applying the pulsed laser holography, the conditions in the measuring volume during the very short exposure time are recorded three dimensionally on the holographic plates. The holograms contain the information about macroscopic structures such as the break up length and the spray angle of the liquid veil near the nozzle and microscopic structures such

as size, position and velocity of the droplets further downstream. The recorded holograms can be reconstructed by means of a continuous laser beam and analysed any time later. The holographic reconstructions can be observed directly or with the help of a microscope lense mounted on a videocamera. The obtained images are delivered to an image processing system.

The main problem appearing in the evaluation of holograms consists in selecting and classifying well-focussed particles while the videocamera scans the three-dimensional holographic image. An aim of this work is to describe an approach to evaluate pulsed laser holograms of particle fields and to reconstruct the spray and its velocity field three dimensionally on a computer. In this study, two off-axis holograms of sprays in an angle of 90° to each other have therefore been recorded.

This paper presents two computer aided procedures to evaluate and reconstruct three dimensionally pulsed off-axis holograms of sprays (single and double pulsed holograms, respectively). They are based on techniques of the digital image processing (IP) and particle imaging velocimetry (PIV) integrated in a personal computer. Using these procedures, the operator is released from the situation of taking decisions interactively during the evaluation process. This allows a more efficient application of drop focussing and classifying criteria, resulting in a substantial increase of the measurements' accuracy and an effective reduction of the time necessery to evaluate the holograms.

EXPERIMENTAL FACILITY

The experiments were carried out in the test facility illustrated in Fig. 1. After being degased by an ultrasonic treatment and by boiling, the test fluid is stored in the pressurized reservoir. The pressure can be varied by means of nitrogen in the range of 0.1 to 2 MPa. The liquid can be heated by three electrical heaters of 1.2 kW each. From an outlet in the lower part of the vessel the fluid is led through an oil heated heat exchanger for a fine adjustment of its temperature and then to the nozzle. The test section itself consists of a coflowing vertical wind tunnel capable of providing air velocities up to 50 m/s and temperatures up to 600°C. In order to make the experimental chamber optically accessible, it is made of a glass-octagon with an inside diameter

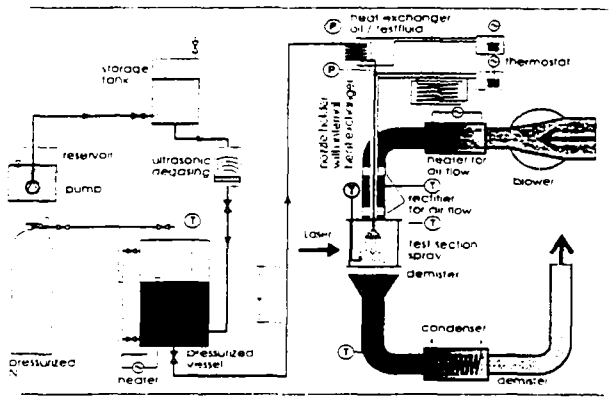

Figure 1: *Test facility*

of 300 mm and a height of 250 mm. The chamber was designed for atmospheric pressure. The nozzle, concentric with respect to the surrounding air flow, can be moved axially to allow the observation of any section of the spray. Downstream the test section, the mixture of air, test fluid and vapour is cooled down in a heat exchanger. The condensate is separated in a demister and collected. Measurements of temperature and pressure at different points of interest in the facility are carried out by conventional thermocouples and pressure sensors monitored by a personal computer.

THE HOLOGRAPHIC TECHNIQUE

The root of the word holography lies in the greek language and describes the ability of the method to record the totality of the light information scattered by or reflected on an object, namely the amplitude or intensity and the phase distribution. A deeper insight into this technique can be found in the literature (LEITH & UPATNIEKS [6], KIEMLE & RÖSS [5]).

Recording of the holograms

The pulsed laser holography, applied in this work represents one of the more suitable non invasive measuring techniques to study the transport phenomena (e.g. heat and mass transfer) in dispersed transparent flows. Three dimensional pictures of the whole volume of interest are taken. Due to the very short exposure time of about 30 ns, even fast moving particles are imaged sharply. In this study, two three dimensional images, perpendicular to

each other. are taken. A scetch of the optical setup is given in Fig. 2.
A pulsed ruby laser generating light pulses with an energy of 1 *Joule* for the very short time of 30 *ns* is used to record the holograms. This laser is operated either in single or in double pulse mode. In single pulse mode the resulting holograms contain macroscopic information about the geometry of the spray. the break up of the liquid sheet. and microscopic data like the droplet diameter and spatial droplet distribution in the control volume. In addition to that. the information of the droplets' velocities and trajectories is obtained by operating the laser in double pulse mode. In this case. two sucsessive conditions of the spray are recorded on each holographic plate without any restriction to the depth of the focus range. With the knowledge of the pulse separation. which can be varied from 1 to 800 μs. and the measured distance between the two successive images of one droplet. the velocity of each droplet is calculated. After being collimated by pas-

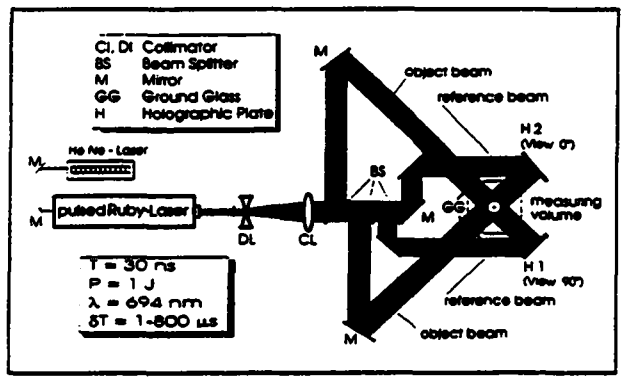

Figure 2: *Optical setup of the holographic camera*

sing two lenses (DL, CL). the laser beam is split into two object beams and two reference beams in the bank of beamsplitters (BS). The object beams are diverted at the mirrors in a way that they cross the test section perpendicular to each other after having been converted into diffuse light at a plate made of ground glass (Fig. 2). Exiting the test section. the object beams fall perpendicularly onto the holographic plates. In contrast to that. the reference beams are directly diverted to the holographic plates. The superposition of the object beam and the reference beam results in an interference figure which contains the whole optical information and is stored on the holographic plate. Applying this measuring technique. particles with a diameter greater than ten times the wavelength of the laser light are imaged sharply. It yields two 3-D images of the spray. recorded simultaneously. without any restriction to the depth of focus range. The principal features of this measuring technique are explained more detailed in MAYINGER [7]. CHAVEZ [2]. and GEBHARD [3].

Reconstruction of the holograms

The holograms are reconstructed by means of two continous HeNe-Laser with a wavelength of 632 nm. simulating the reference beams during their recording. By illuminating the holographic plates with these continous laser beams. the real images of the recorded scenes are formed three dimensionally. The images are reconstructed simultaneously and recorded by two Newicon TV-cameras. so that two views of the spray perpendicular to each other are obtained. They represent two three-dimensional (3-D) images corresponding to one "frozen" scene of the spray. as illustrated in Fig. 3. Because the video camera only can take two-dimensional (2-D) pictures. that is its optical plane. it must be focussed stepwise along the depth coordinate in order to record the entire 3-D information contained in the holographic image. Therefore the test section was devided into several subvolumes with the dimension of $4 \times 4 \times 2\ mm^3$. corresponding to the field of view and the depth of field of the observing cameras. In this manner. the 3-D holographic reconstructions are transformed into a series of 2-D video images. In order to control the position of the cameras each camera is mounted on a traversing mechanism. which is controled by a computer. The optical information contained in the reconstructed images is scanned by the video cameras and transmitted to the digitizer. The signal is transformed into digital information and then stored in the digitizer frame memory in form of an array of 512 x 512 picture elements (pixels) of 8 bits. A bus interface directly connects the digitizer to the host computer. The processing of the digitized picture is then carried out by the host computer using the digitizer frame memory interactively for pixel allocation. In order to visualize the information stored in the digitizer frame memory. it produces a continuous RGB

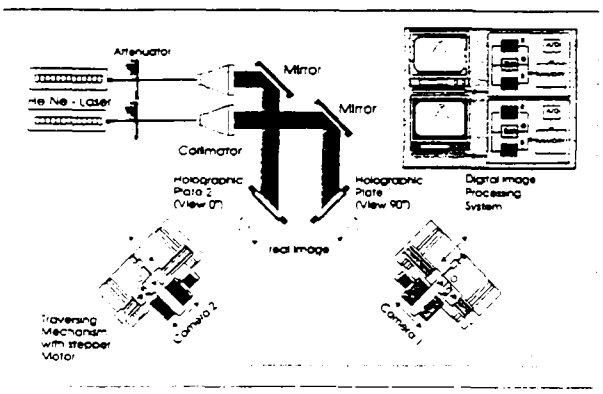

Figure 3: *Optical setup for the reconstruction and scanning of the holograms*

(false color: red, green, blue) output signal which can be seen on the graphics monitor (Fig. 3).

HOLOGRAM EVALUATION

One of the principal problems appearing in the application of pulsed laser holography consists in handling the large amount of information stored in the holograms. Theoretically, holographic materials are able to store the information about position, texture and brightness of more than 10^6 particles per square millimeter. Though in this study the droplet concentration was much lower (less than 10 drops per cubic millimeter), one single hologram still can contain the information about position, size, and velocity of thousands of droplets. Comprehensive studies of the characteristics of the droplets and the interactions with their gaseous environment necessarily require the help of computer-aided particle counting and measuring methods.

Single pulsed holograms

Representative stages of the image processing are presented exemplarily in form of photographs in Fig. 4 (CHAVEZ [2]). The nozzle is included for better orientation. The first modulus of the software transforms the original image (A), seen by the videocamera into a binary image. This original image of a holographic reconstruction is smoothed (B) and treated with a gradient filter (C). Sharply imaged structures are detected, edged and filled. Finally the image is binarized (D). An additional tool in this modulus allows to analyse either the big structures like the liquid veil (E, above) or only the smaller structures like the droplets (E, below). These pro-

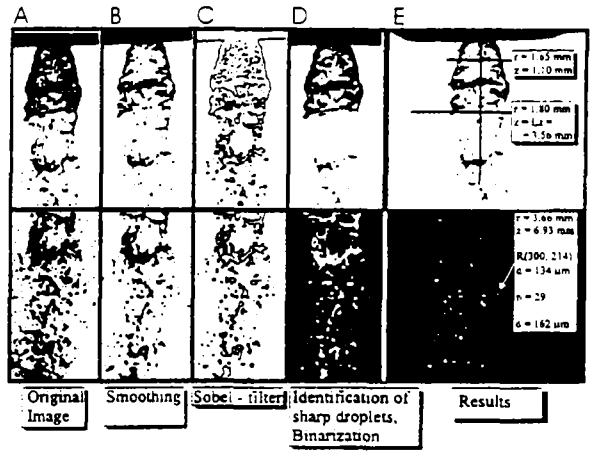

Figure 4: *Representative steps of image processing of a slice cutted from a holographic reconstruction*

cedures are performed by stretching the histogram of the grey values of the image and the application of a threshold filter with values obtained from that histogram. As a result, binary coloured images are obtained, which are the basis for the following evaluation algorithms. During the calibration of the optical system it was observed, that the radial and the tangential error of distortion of the used microobjective lenses (Nikkon 105 *mm*) was less than one single pixel on the surface of the camera chip. This error was assumed to be negligibly small. A comprehensive description of hologram evaluations by applying digital image processing can be found in CHÁVEZ & MAYINGER [1].

To reconstruct the recorded condition three dimensionally, both views of this condition have to be correlated. The droplets differ in size and shape, but this feature-based matching is a weak criterion to correllate both views because of the influence of the illumination and the variation of the the droplets' shape between both views. Generally the experience shows, that more than two views are needed to determine the particles' positions sufficiently accurate due to the large number of ambiguities (physical possible matches), if this feature based matching criterion is applied.

A second modulus of the software was developed

to be able to perform the matching with only two views. the stereomatching algorithm. It determines the droplets' positions in space from the binary pictures by applying the focussing criterion. The physical model used in the stereomatching process is illustrated in Fig. 5. As explained above. the

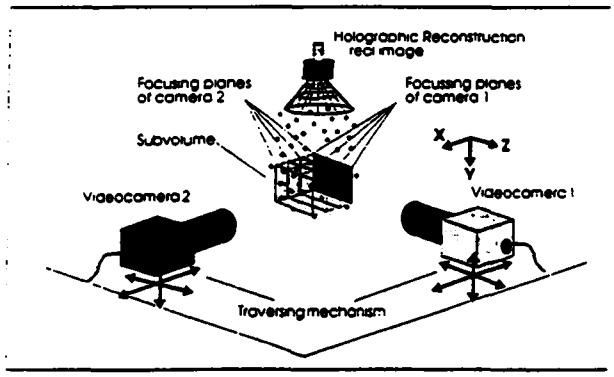

Figure 5: *Physical model of the stereomatching*

depth coordinate of a droplet in one view is known within the small range of the depth of field of the observing camera. With the agreement of the Y-coordinate in both views, this is the second criterion needed to determine the droplet's exact position in the second view. The determination of the droplets' positions is performed by a coordinate transformation having the knowlege of their Y-position and the depth of the focussing plane of the observing cameras, regardless of any feature-based criterion.

Double pulsed holograms

The information about the droplets' velocities and trajectories is obtained from double pulsed holograms. The holograms contain a conglomeration of spot couples. Each couple represents one spray droplet imaged twice at two successive positions corresponding to the time interval ($1 - 800\mu s$) between the two exposures to the laser light. In order to evaluate the double pulsed images, a routine VEL was developed. Its task is to identify the spot couples from the pictures taken by each camera. to measure the distance between the center points of the two images. and to compute the droplets' trajectories related to the focussing plane of the observing camera. without taking into account the particles' off-plane velocity. The routine consists of two moduli: a spatial frequency analyzer and a measuring algorithm. The different steps of the evaluation of double pulsed hologram by aplying the moduli of the routine VEL is illustrated in Fig. 6. Firstly, the image is binarized as described above. With no regard the shape and with the assumptions that the picture was obtained from a double pulsed holographic reconstruction. and that the depicted elements (6A) represent droplets which are moving along the Y-axis within a guessed angle of $\pm 45°$, the first modulus recognizes automatically the two postions of each droplet. Firstly, the coordinates of the spot center points S_1. S_2. and the vectorial distance $\vec{d}$ between each two center points are calculated. The vectorial distance $\vec{d}$ can be split into a distance d and an angle β towards the vertical. Then a frequency analysis converts the spatial distribution of β into a normalized frequency distribution with the maximum F_{max} used as a norm (6B). With the information of this preferential angle. a second frequency analysis with the distance d as the independent variable is carried out (6C). The preferential angle β_p and the preferential distance d_p appear as peaks in the diagrams and form the mean velocity $\bar{v}$.

This algorithm is applied to both views and an average velocity projected into the focal planes of the cameras is obtained. Evaluating the mean velocities $\bar{v}$ in both views. the real angle in space, called β_r. which consists of an cylinder coordinate Φ and the angle β_r is calculated.

To get the real velocity in space. a second modulus was developed for the subroutine VEL. Both the the magnitude d_p of $\bar{v}$ with a tolerance of $\pm 0.1 d_p$ and its corresponding angle β_r with the tolerance of $\pm\beta_0$, which can be varied between 7 and 15° were incremented. The chosen tolerances allow strong variations of the droplet trajectories. Using these variations the algorithm creates a search volume to find the second position of a droplet (6D). Herein V_i and β_i are the real magnitude and direction of the velocity corresponding to the imaged positions of the droplet. respectively. At least 75% of the couples are detected and measured. aplying the moduli of the subroutine VEL (6E). The trajectories obtained by applying both moduli of VEL for the droplets of a spray generated by a hollowed cone nozzle are shown in Fig. 7. This algorithm is highly reliable because of the found unidirectional flow of the droplets with respect to the analyzed volume.

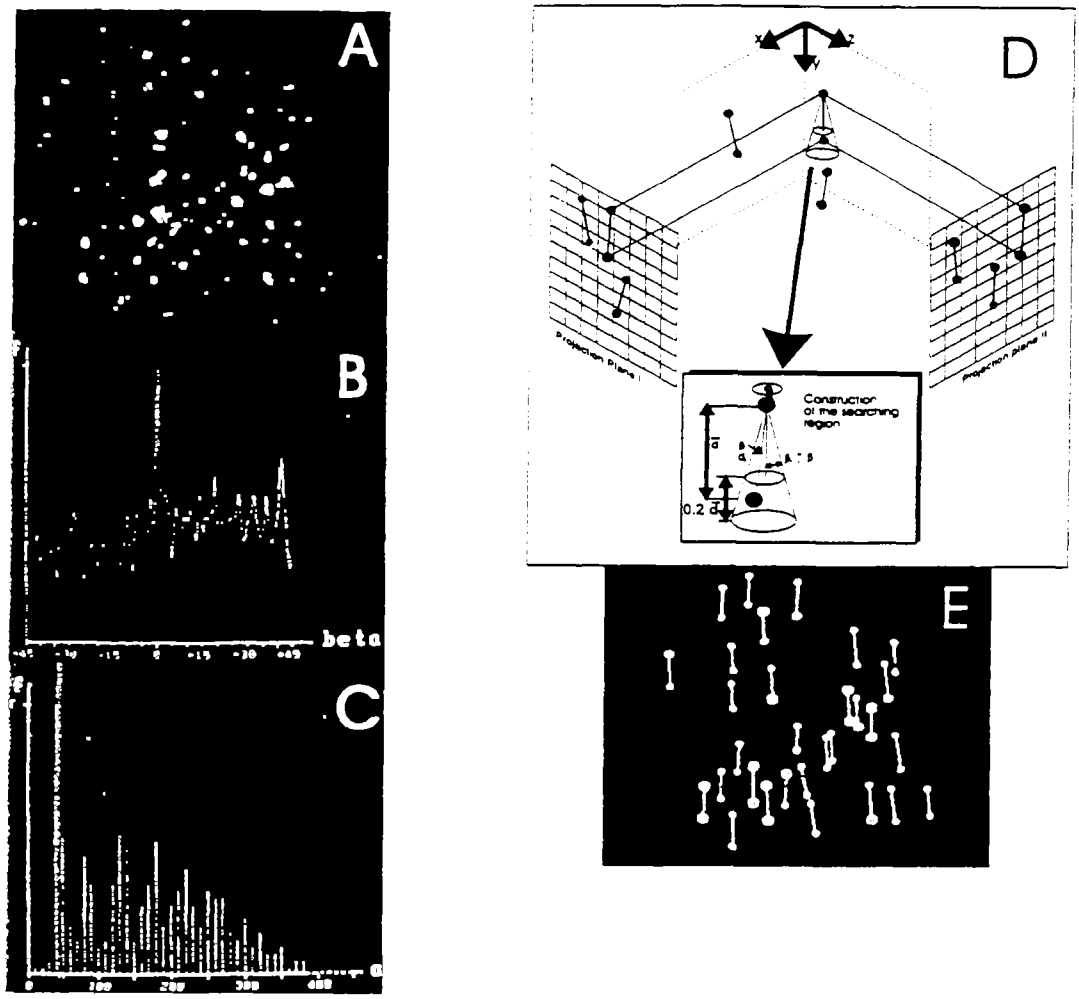

Figure 6: *The moduli of the routine VEL*

RESULTS AND DISCUSSION

As an example of the applicability of the discussed recording and evaluation technique, the results obtained at a flat spray nozzle with an elliptic orifice (main axis: $1.19 \times 0.49\ mm$) are presented in the following. The injection pressure of the test fluid – distilled, degased water – ranged from 0.025 to 0.8 MPa and the temperature from $20°C$ (subcooled liquid) up to $150°C$ (superheated with respect to the pressure in the test autoclave of 0.1013 MPa, GEBHARD [3]).

Mechanism of the disintegration

Holographic reconstructions of a superheated injection jet and their binarized images are shown exemplarily in Fig. 8 for different injection conditions. By means of these images the two driving mechanisms of the disintegration of a superheated liquid jet can be explained: the sheer stress between the liquid and the adjacent gasous phase, and the liquid's evaporation. In case of a superheat of up to 10 K, infinitesimal small transient sheer stresses cause oscillations increasing in amplitude along the liquid veil. These oscillations lead to the separation of unstable ligaments disintegrating to stable droplets further downstream (A). At this low superheat, the activation rate of nuclei is not high enough to have a noticeable influence on the disintegration process. Rising the superheat results in

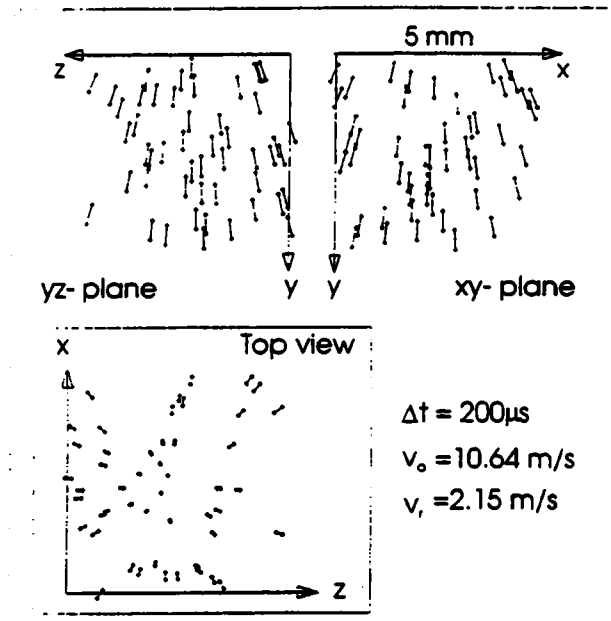

Figure 7: *Trajectories of the droplets of a spray formed in a hollowed cone nozzle*

a higher activation rate of these heterogen generated nuclei. These nuclei form growing vapour bubbles causing perforations in the veil. Due to surface tension forces, these perforations grow with the distance from the nozzle, yielding in the separation of ligaments. These ligaments disintegrate independently from the remainig veil (B,C). If the superheat exceeds $40K$, the very high activation rate of the nuclei results in an immediate flash evaporation of the liquid exiting the nozzle (D,E).

Macroscopic Structures

The shape of the liquid veil is characterized by the breakup length L_z and the spray angle α. It determines size, distribution, and velocity of the generated droplets. A spray can be subdivided into three zones:

- the continuous liquid veil zone, formed by the test fluid exiting the nozzle.
- the breakup zone, where the veil is disintegrated and the droplets are generated.
- and the droplet zone itself.

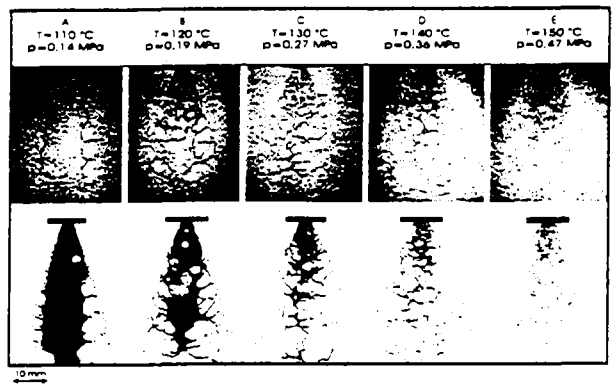

Figure 8: *Influence of different injection conditions on the spray.*

The breakup length L_z, i. e. the distance between the nozzle and the breakup zone, is plotted against the injecton pressure for different temperatures in Fig. 9A. Subcooled conditions are represented by solid lines, superheated conditions are represented by dashed lines. For subcooled conditions, L_z increases with the pressure. After reaching a maximum it decreases again. The liquid is disintegrated due to the sheer stress as explained above. By increasing the temperature the viscosity and the surface tension of the liquid is decreased. This results in an increase of the breakup length. The appearance of slightly superheated spray is similar to those of subcooled sprays. Increasing the pressure leads to a higher velocity and greater sheer stress. Therfore the breakup length decreases in the high pressure range. In the range of app. 120 to 130°C, the breakup length increases with the injection pressure because of the higher initial velocity of the liquid. Rising the temperature enhances the acivation rate of the nuclei. This yields in a decrease of the breakup length. If the injected liquid is highly superheated, the veil disintegrates directly after exiting the nozzle. In this case, the breakup length L_z is not a function of the pressure. The sprayangle α is depicted against the pressure for different temperatures of the injected liquid in Fig. 9B. For subcooled injection (dashed lines), the spray angle α increases with the injection pressure and reaches a borderline asymptotically. The influence of the temperature on the spray angle is small for injection pressures up to 0.4 MPa and negligible for higher injection

pressures. In contradiction to that the spray angle

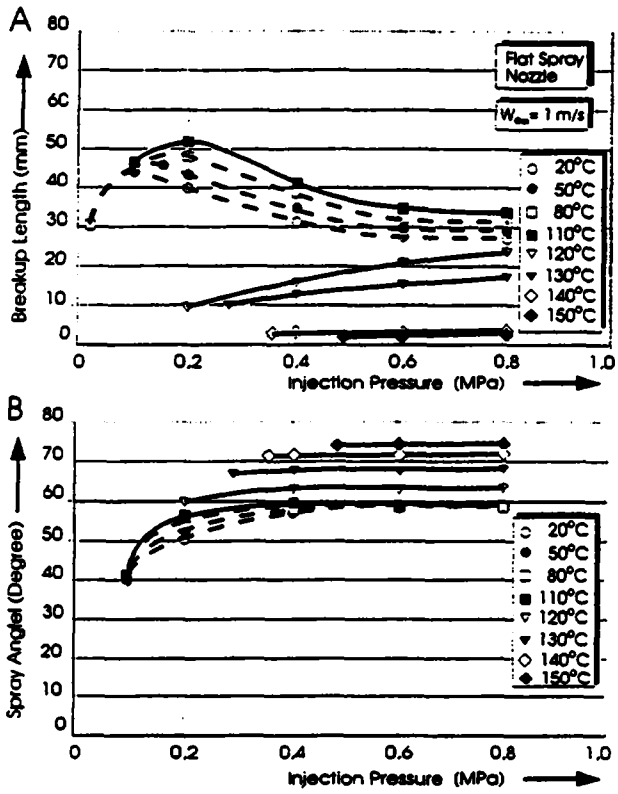

Figure 9: *Breakup length and spray angle as a function of the injection pressure for different temperatures of the test fluid.*

is higly depending on the temperature for superheated liquid. Higher injection temperatures cause an increase of the spray angle because of the enhanced activation rate of the nuclei and thus the stronger flashing of the injected liquid.

Microscopic Structures

From the analysis of the macroscopic strutures of the different sprays it can be drawn that for any injection condition the disintegration process is completed at an axial distance of $Y = 80mm$ from the orifice. Therefore, the results of the analysis of the sprays' microscopic structures presented in the following refer to that Y-coordinate. The found diameter of the droplets is summarized in form of their Sauter Diameter as a function of the injection pressure for different temperatures in Fig. 10.

If subcooled or slightly superheated water is injected, the droplets' Sauter diameter strongly decrease with a higher injection pressure. Increasing the injection pressure to more than $0.6MPa$ only has a small effect on the Sauter diameter of the generated droplets. Raising the pressure results in a higher velocity of the liquid and thus in higher inertial forces and sheer stresses on the veil yielding in its better disintegration. For higher temperatures in the subcooled region and for slightly superheated liquid, the size of the droplets decreases because of the lower viscosity of the liquid.

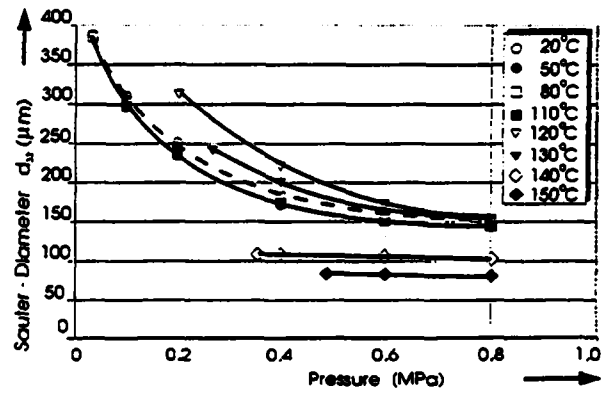

Figure 10: *Sauter diameter as a function of the injection pressure at different temperatures of the test fluid.*

For a superheat of more than 10 K, the generating of vapour bubbles becomes the dominating effect of disintegrating the liquid veil. In the temperature range from app. 110 $°C$ to 130 $°C$ the separation of ligaments from the veil can be observed. In this temperature range, the liquid sheet in the breakup zone and thus a separated ligament is thicker than the wavy sheet obtained by injecting subcooled water. This yields in an increase of the Sauter diameter of the generated droplets. If the injected liquid is strongly superheated, the jet is flashed into the test section. A fine spray with a small Sauter diameter of the generated droplets is obtained. This effect can be enhanced by a further increase of the liquid's temperature. In this temperature range, the influence of the injection pressure on the Sauter diameter is very low.

The radial distribution of the droplets' diameter

80mm downstream the orifice is given in Fig.11 for a injection pressure of 0.4 MPa. As it can be seen, the increase of the temperature of the liquid leads to a more uniform distribution of the diameter.

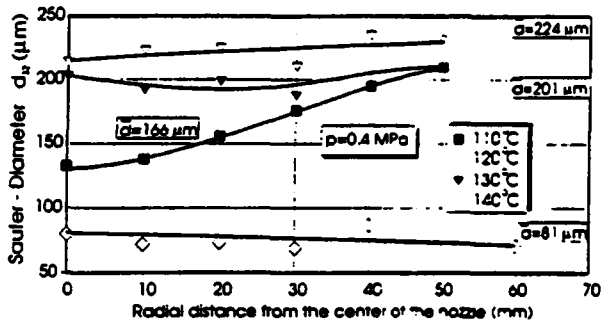

Figure 11: *Sauter diameter as a function of the radial distance from the center of the nozzle.*

In Fig. 12, the velocity of subcooled jet is plotted against the axial distance from the orifice for different injection pressures at a temperature of 50°C. The velocities were derived from the evaluation of double pulsed holograms.

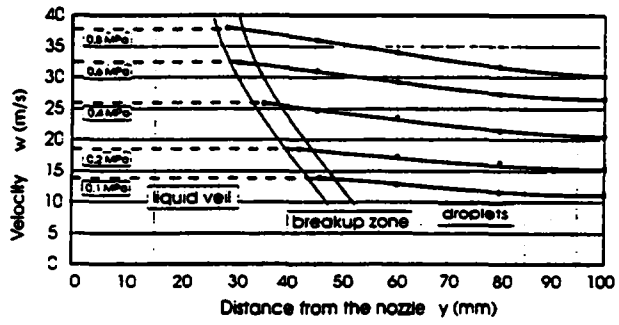

Figure 12: *Velocity of the liquid veil and the droplets of a subcooled injetion jet.*

The velocities of the liquid veil was determined by measuring the displacement of specific characteristics in the veil. As it can be seen in Fig. 12, the veil's velocity increases and its length decreases with the injection pressure. Its velocity is constant within 5 % . When the droplets are generated, their velocity decreases with the axial distance due to friction. The smaller droplets, generated at high injection pressures, tend to slow down faster and lose a higher percentage of their initial velocity than the bigger droplets generated at low injection pressures.

The velocity of the droplets of a superheated spray were determined at an axial distance of 80 mm from the nozzle. They are plotted - classified in two diameter classes - for four radial locations in Fig 13. Their velocity decreases with the radial distan-

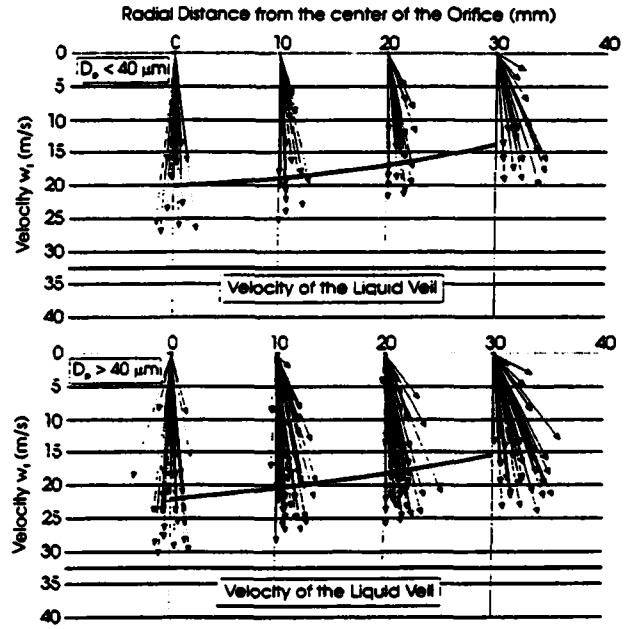

Figure 13: *Velocity of different droplet classes at an axial distance of 80 mm from the nozzle.*

ce from the center due to the higher impact of the friction. Big droplets move faster than small droplets because of their higher inertia. The average velocity of the droplets is included in Fig. 13 in form of a solid line to illustrate the loss of the velocity of the droplets compared to that of the liquid veil.

Accuracy

The main source of uncertainty of this measuring technique was found to be the pixel representation of circular objects (droplets), especially if these objects are represented by less than 10 pixels (independent of the absolute pixel size). The resolution of the area measurement tool in the developed code was set to 5 pixels, resulting in the maximum error of ±3% for areas with sizes between 6 and 40 pixels. In this work, the sizes of the droplets' images ranged between 14 pixels ($\circ$ 30 μm) and 148 pixels ($\circ$ 310 μm) pixels. The error in imaging larger objects or structures was found to be less than 1%.
The determination of the velocity of one droplet depends on the quality of the stereomatching and the yield of the found couples. Due to the fact of taking into account thousands of droplets, their mean velocity can be calculated with the high accuracy of ±5%.

CONCLUSION

In this study, a 3-dimensional particle imaging velocimetry technique is presented, which is based on the evaluation of pulsed laser holograms. The large amount of data, stored in a hologram, can be analysed correctly without previous knowledge of the flow in the measuring volume. The code works with the high accuracy of ±3% for the determination of the droplets' sizes and ±5% for the determination of their mean velocity. It can be integrated into a simple digital image processing system with common digitizers (512×512 pixels, 8 bit depth). The application of this technique allows to analyse both macroscopic structures such as the dimension of the liquid sheet and microscopic structures such as the droplets' sizes and velocities.

ACKNOWLEDGEMEENT

This work was funded by the Deutsche Forschungsgemeinschaft.

References

[1] Chavez, A. & Mayinger, F.,(1992) Measureament of the direct-contact condensation of pure saturated vapour on an injection spray by applying pulsed laser holography. Int. J. Heat Mass Transfer. Vol. 35, No. 3, pp. 691-702

[2] Chavez, A.,(1991) Holographische Untersuchung an Einspritzstrahlen: Fluiddynamik und Wärmeübergang durch Kondensation. Diss. TU München

[3] Gebhard, P.,(1996) Zerfall und Verdampfung von Einspritzstrahlen aus lamellenbildenden Düsen. Diss. TU München

[4] Hausmann, G. & Lauterborn, W., (1980), Determination of size and position of fast moving gas bubbles in liquids by digital 3-D image processing of hologram reconstructions, Applied Optics, Vol. 19, No. 20, pp. 3529-3535

[5] Kiemle, H. & Röss, D. (1969), Einführung in die Technik der Holografie. Akademische Verlagsgesellschaft, Frankfurt a. M.

[6] Leith, E.N. & Upatnieks, J. (1964), Wavefront reconstruction with diffused illumination and three dimensional objects. J. Opt. Soc. of America. Vol. 54, No. 11, 1195-1301.

[7] Mayinger, F. (1994). Optical measurements - Techniques and application, Springer Verlag